Antimonides T2SL Mid-Wave and Long-Wave Infrared Focal Plane Arrays for Earth Remote Sensing Applications

Sarath Gunapala, David Ting, Sir Rafol, Alexander Soibel, Arezou Khoshakhlagh, Sam Keo, Brian Pepper, Anita Fisher, Cory Hill, and Thomas Pagano
Center for Infrared Photodetectors, Jet Propulsion Laboratory, California Institute of Technology
Pasadena, California, USA

Paul Lucey, Robert Wright, Miguel Nunes, and Luke Flynn
Hawai'i Institute of Geophysics and Planetology, University of Hawai'i at M noa, Honolulu, Hawaii, USA

Sachidananda Babu and Parminder Ghuman
NASA Earth Science Technology Office
Greenbelt, Maryland, USA

ABSTRACT

In this invited paper, we will report our recent efforts in achieving high performance in Antimonides type-II superlattice (T2SL) based infrared photodetectors using the barrier infrared detector (BIRD) architecture. The initial BIRD devices (such as the nBn and the XBn) used either InAs absorber grown on InAs substrate, or lattice-matched InAsSb alloy grown on GaSb substrate, with cutoff wavelengths of ~3.2μm and ~4μm, respectively. While these detectors could operate at much higher temperatures than existing MWIR detectors based on InSb, their spectral responses do not cover the full (3 – 5.5μm) MWIR atmospheric transmission window. The T2SL BIRD devices not only covers the full MWIR atmospheric transmission window, but the full LWIR atmospheric transmission window and beyond. The LWIR detectors based on the BIRD architecture has also demonstrated significant operating temperature advantages over those based on traditional p-n junction designs. Two 6U SmalSat missions CIRAS (Cubesat Infrared Atmospheric Sounder) and HyTI (Hyperspectral Thermal Imager) are based on JPL's T2SL BIRD focal plane arrays (FPAs). Based on III-V compound semiconductors, the BIRD FPAs offer a breakthrough solution for the realization of low cost (high yield), high-performance FPAs with excellent uniformity and pixel-to-pixel operability.

Keywords: type-II superlattice, infrared detector, quantum efficiency, digital, focal plane array

1. INTRODUCTION

Realization of unipolar barrier infrared detector structures typically involves a set of rather stringent requirements. Designing an nBn IR detector requires a matching pair of absorber and barrier materials with the following properties: (1) their valence band edges must be approximately the same to allow un-impeded hole flow, while their conduction band edges should have a large difference to form an electron barrier, (2) the absorber should have the desired band gap, (3) the absorber should be very closely lattice-matched to the substrate to ensure high material quality and low defect density, and (4) the barrier should also be approximately lattice-matched to the substrate, although the requirement here is less stringent since a barrier thickness of 1,000 to 2,000 Å is typically sufficient, and therefore a modest amount of strain can be tolerated. The conditions favorable for constructing nBn structures are found in the nearly lattice-matched semiconductors of InAs, GaSb, and AlSb, commonly referred to as the 6.1 Å material system since InAs,

GaSb, and AlSb all have lattice constants of approximately 6.1 Å. They are also commonly referred to as the antimonides (InAs is included by virtue of being closely lattice-matched to GaSb and AlSb). BIRDs have been demonstrated using electron unipolar barriers with MWIR and LWIR antimonides superlattices to achieve near diffusion limited performance. In general, there are many types of antimonides based superlattices such as InAs/GaSb, InSb/InAsSb, InSb/InAs, InAs/InAsSb, etc. Experiments with all these potential T2SL material system has culminated the InAs/GaSb and InAs/InAsSb based BIRDs. The InAs/InAsSb strained layer superlattice (SLS) is simpler to grow by molecular beam epitaxy. The MBE growth of InAs/InAsSb SLS involves only turning on and off the Sb shutter, as compared to the use of four shutters sequence in the InAs/GaSb superlattice. Whereas the growth of the InAs/GaSb superlattice is considerably more complicated, which involves strain-balancing interfaces necessary to achieve good material quality. In general, InAs/InAsSb SLS has longer minority carrier lifetimes. There has also been some evidence suggesting that the InAs/ InAsSb SLS is more defect tolerant, because, the energy levels for the SRH defect centers are in resonant with the conduction band rather than in the middle of the bandgap where they can contribute to the carrier recombination (G-R) process [1-3]. It's worth noting that, BIRDs have been implemented for bulk InAs, InSb, InAsSb, InGaAsSb, InAsPSb, and HgCdTe as well.

2. BARRIER INFRARED DETECTOR (BIRD)

The InAs/InAsSb SLS has ease of growth and minority carrier lifetime advantages, while InAs/GaSb SL holds optical and hole transport property advantages. The choice between the two material systems depends on the cutoff wavelength, growth, and processing capabilities. The InAs/InAsSb SLS appears to be the most effective when implemented in the MWIR, where it could have an advantage over the InAs/ GaSb SL. The general concepts of InAs/InAsSb SLS unipolar barrier infrared detectors (BIRDs), MWIR detector, and FPA results has been previously described [1]. Below, we present the electrical (Figure 1) and optical (Figure 2) characterization results from a previous InAs/InAsSb SLS MWIR BIRD.

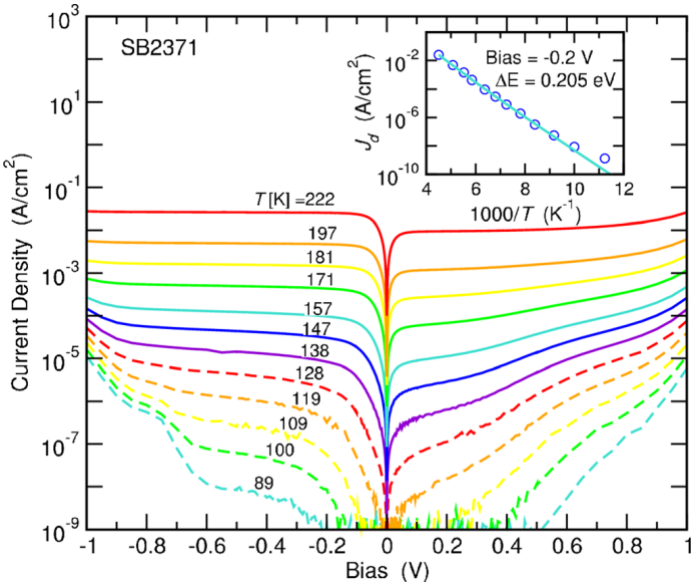

Figure 1. Dark current density (J_d) as a function of applied bias, measured at temperatures ranging from 89K to 222K. The inset shows temperature dependence of J_d (over the same range as the main plot) at -0.2 V bias. (Taken from reference 3)

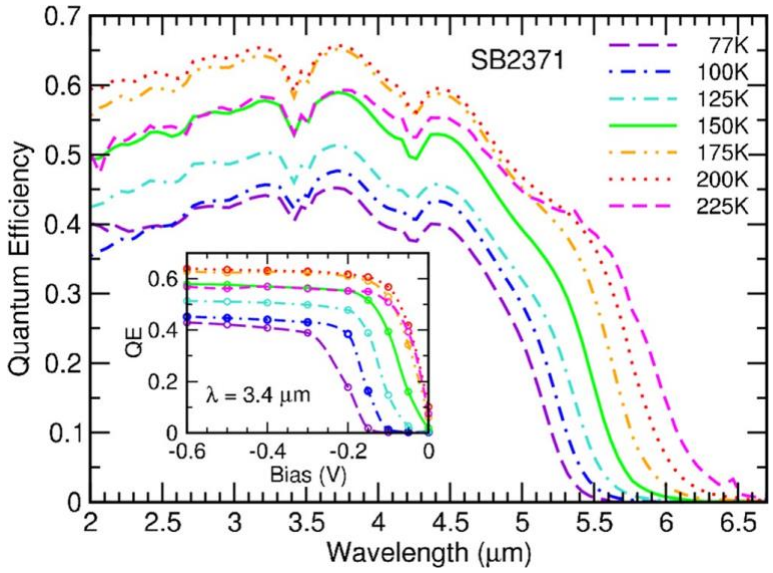

Figure. 2. Backside illuminated spectral quantum efficiency (QE) for an MWIR detector measured at temperatures ranging from 77 K to 225 K. The inset shows the QE measured at 3.4 μm as a function of applied bias at the same set of temperatures (Taken from reference 3)

Due to the ease of fabrication and aforementioned results the InAs/InAsSb (Gallium-free) T2SLS has emerged as an alternative adjustable bandgap, broad-band III-V IR detector material to the more established InAs/GaSb type-II superlattice (T2SL). Furthermore, the T2SLS material can be grown on InAs or GaSb substrates, and GaSb wafers are available in 2", 3", 4" and 6" diameters.

3. MWIR T2SL BIRD FOCAL PLANE ARRAY FOR CIRAS

Hyperspectral radiances measured from Low Earth Orbiting (LEO) infrared sounders including the NASA Atmospheric Infrared Sounder (AIRS) on Aqua, and the Cross-track Infrared Sounder (CrIS) on the Joint Polar Satellite System (JPSS) have among the highest impact of any measurement type when assimilated into operational weather forecast models. LEO IR sounder radiances are used to retrieve temperature and moisture profiles with high vertical resolution. These profiles have been used to validate water vapor distributions in climate models and confirm positive water vapor feedback to global warming. CubeSat Infrared Atmospheric Sounder (CIRAS) is an instrument approach to achieve temperature and water vapor profiles using hyperspectral infrared in a 6U CubeSat [4]. The CIRAS is designed with a high operating temperature (HOT) MWIR BIRD FPA developed at JPL.

An InAs/InAsSb SLS BIRD structure was grown on a 4-inch diameter low Te-doped GaSb (100) substrate in a Veeco Applied-Epi Gen III molecular beam epitaxy (MBE) chamber to fabricate a MWIR FPA for CIRAS instrument. The BIRD architecture is used for G-R and surface-leakage dark current suppression. Square mesa photodiodes of area 250μm x 250μm were fabricated along with detector arrays for responsivity and dark current measurements. The devices were not passivated nor treated with anti-reflection coating. Figure 3 shows the dark current density as a function of bias voltage. Figure 4 shows the spectral QE derived from back-side illuminated (through the GaSb substrate) spectral responsivity measured at temperatures ranging from 40K to 80K; the QE has not been corrected for substrate reflection or transmission. Accordingly, the spectral QE for 77K and 150K was taken at -30mV. The cutoff is 5.7μm at 120K which the QE is 50% of of the QE maximum.

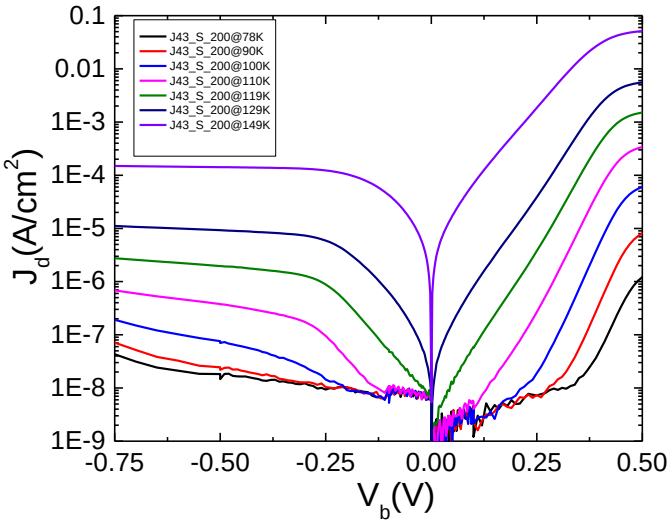

Figure 3. Dark current density (J_d) as a function of applied bias, measured at temperatures ranging from 78K to 149K.

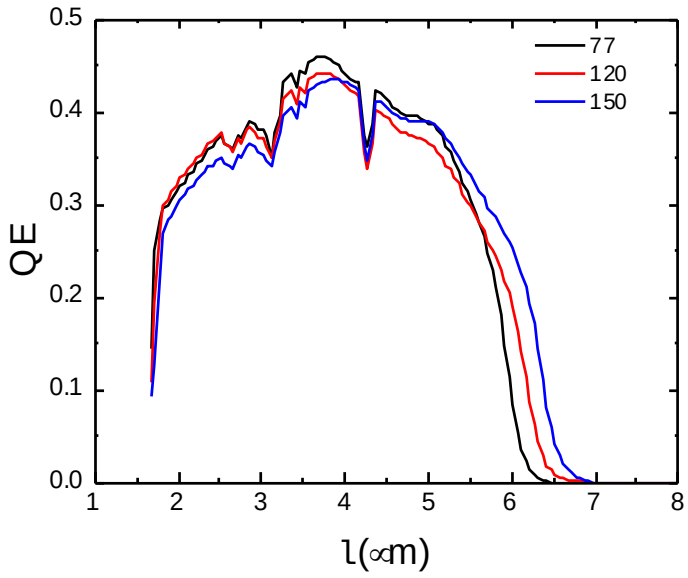

Figure. 4. Backside illuminated spectral QE (no A/R coated) of the CIRAS MWIR detector measured at temperatures ranging from 77K to 150K.

CIRAS uses a 512 x 640 element 24 μm pitch JPL High Operating Temperature Barrier Infrared Detector (HOT-BIRD) FPA. The HOT-BIRD technology is based on III-V compounds and offers a breakthrough solution for the realization of lower dark current and improving uniformity and operability compared to II-VI material (MCT) at lower cost. Low 1/f noise and high temporal stability allows CIRAS to use a slow scan

for better sensitivity and less frequent calibrations10. Figure 5 shows the FPA net QE at the 3-5 μm spectral band. Figure 6 shows an image taken using the CIRAS HOT-BIRD detectors. This image reflects the high operability and good sensitivity of the device. The Readout Integrated Circuit (ROIC) chosen for the CIRAS detector was the SBF193 by Lockheed Martin. 56 FPAs, consisting of the detector hybridized to a ROIC, were successfully fabricated on the first lot demonstrating the high producibility of the process. Of these 5 were delivered for substrate removal and testing. The FPA chosen to be placed in the IDCA for CIRAS was serial number 17CIL35. The FPA exhibits good connectivity at room temperature with very few poorly connected pixels. The FPA was tested at two operating temperatures 130K and 115K. The CIRAS FPA performance requirements and expected capability are shown in Table 1.

Detector	Requirement	Expected Capability	Rationale
Pixel Size (μm)	24±1	24	SBF-193 ROIC ICD
Spectral Range (μm)	4.08-5.13±1%	2 – 5.5	FPA result
Quantum Efficiency (%)	> 62	~40	FPA result
Operability	> 0.95	> 0.999	FPA result
Dark Current (A/cm^2)	<7.57e-07	< 3e-07	FPA result
Frame Rate (Hz)	30.0±10%	< 88 (max)	SBF-193 ROIC ICD
ROIC Saturation (e-)	> 8e+06	8.4e+06	SBF-193 ROIC ICD
ROIC Noise (e-)	< 600	< 500	SBF-193 ROIC ICD
Operating Temperature	< 115K	115K	Device/FPA result

Table 1: CIRAS HOT-BIRD FPA performance requirements and measurements.

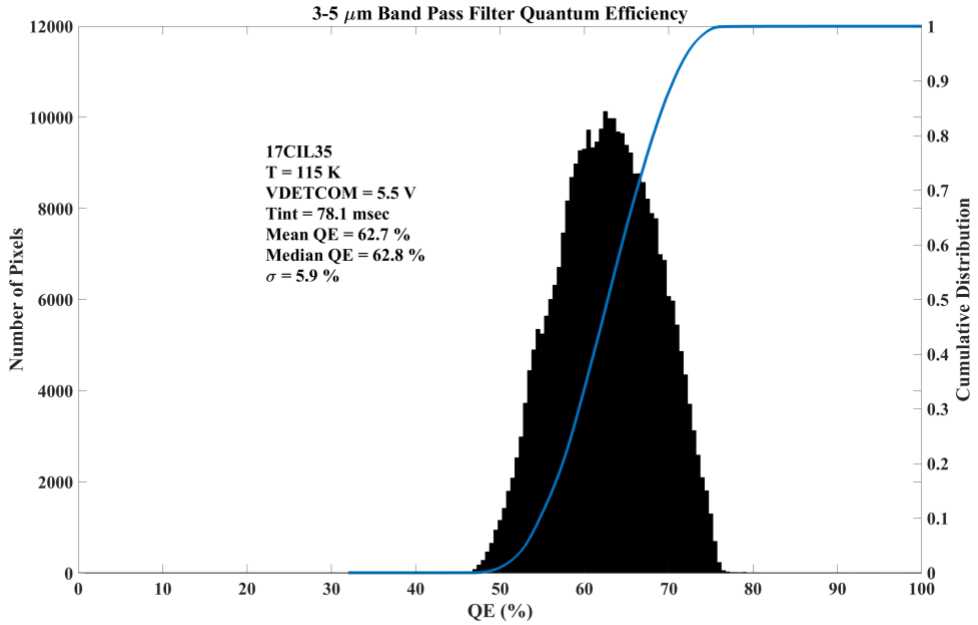

Figure. 5. Backside illuminated spectral QE (no A/R coated) of the CIRAS MWIR detector measured at temperatures ranging from 77K to 150K.

The FPAs are mounted in an evacuated integrated dewar cooler assembly (IDCA). The CIRAS FPA on the dewar cold finger is shown in Figure 7(a) and the completed flight IDCA is shown in Figure 7(b). As

mentioned above the IDCA provides not only the vacuum environment but includes the cryocooler for the detector and cold filters for blocking Ghosting and out-of-band light. The IDCA also includes the proximity board that provides clocks, biases and A/D to the FPA and the camera electronics that provide power and data formatting for the Camera Link output. Early in the design phase we recognized that the grating spectrometer will produce a small amount of ghosting that can introduce spectral mixing of energy in the spectrometer. Cold filters were designed to mitigate the problem and essentially pass only energy for half the spectrum over the corresponding half of the focal plane. One cold filter passes 4.0-4.6 μm and rejects everything out of this band (from 1.5-4.0 μm and 4.6-6.5 μm), while the other filter passes the 4.6-5.2 μm and rejects similar to the other filter. These filters are also mounted on the cold plate directly over the detector and together provide the necessary out-of- band blocking and ghosting reduction required by the system.

Figure 6. An image taken with a MWIR T2SLS BIRD focal plane array.

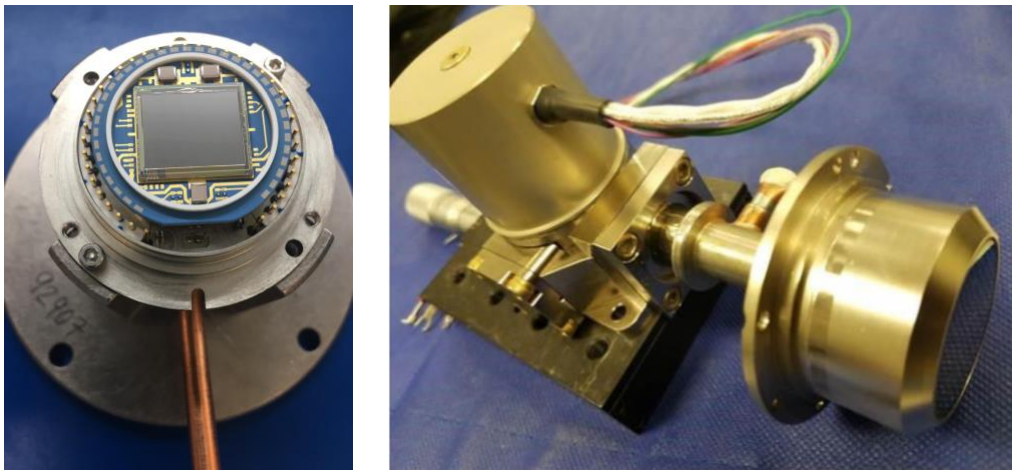

(a) (b)

Figure 7. (a) CIRAS FPA mounted on the dewar cold finger; (b) The CIRAS integrated dewar cooler assembly (IDCA).

4. LWIR T2SL BIRD FOCAL PLANE ARRAY FOR HyTI

The HyTI mission [5], funded by NASA's Earth Science Technology Office InVEST (In-Space Validation of Earth Science Technologies) program, will demonstrate how high spectral and spatial long-wave infrared

image data can be acquired from a 6U CubeSat platform. The mission will use a spatially modulated interferometric imaging technique to produce spectro-radiometrically calibrated image cubes, with 25 channels between 8-10.7 μm, at a ground sample distance of ~70 m. The HyTI performance model indicates narrow band NEΔTs of <0.3K. The small form factor of HyTI is made possible via the use of a no-moving-parts Fabry-Perot interferometer, and JPL's cryogenically-cooled HOT-BIRD FPA technology.

HyTI allows for high spatial and spectral resolution LWIR imaging by combining the multiplex advantage common to all interferometers with the sensitivity of JPL's Barrier Infra-Red Detector FPA technology. Based on III-V compound semiconductors, the BIRD detectors offer a breakthrough solution for the realization of low cost (high yield), highperformance FPAs with excellent uniformity and pixel-to-pixel operability. These antimony (Sb) compound-based BIRD detectors outperform existing thermal infrared detectors including Quantum Well Infrared Photodetectors (QWIPs). To achieve acceptable dark current levels (see below), the FPA must be maintained at a temperature of 68 K. The spectral sensitivity is in the range 8-10.7 μm, with a quantum efficiency of 35%. For HyTI an FPA of 640 Å~ 512 elements will be used. To achieve the required frame rate (139 Hz), the FPA will be windowed, with 320 detectors comprising the image swath (~19 km from a 400 km orbit), and 512 used to sample the interference pattern in the in-track direction. This frame rate allows for oversampling (Å~1.2) in the in-track dimension at orbital velocity.

LWIR detectors based on the BIRD architecture has also demonstrated significant operating temperature advantages over those based on traditional p-n junction designs [6]. An InAs/InAsSb SLS BIRD structure was grown on a 4-inch diameter low Te-doped GaSb (100) substrate in a Veeco Applied-Epi Gen III MBE machine. Square mesa photodiodes of area 250μm x 250μm were fabricated along with detector arrays for responsivity and dark current measurements. These devices were passivated, but not treated with anti-reflection coating at the time of this manuscript preparation. Figure 8 shows the spectral QE derived from back-side illuminated (through the GaSb substrate) spectral responsivity measured at temperatures ranging from 60K to 75K; the QE has not been corrected for substrate reflection or transmission.

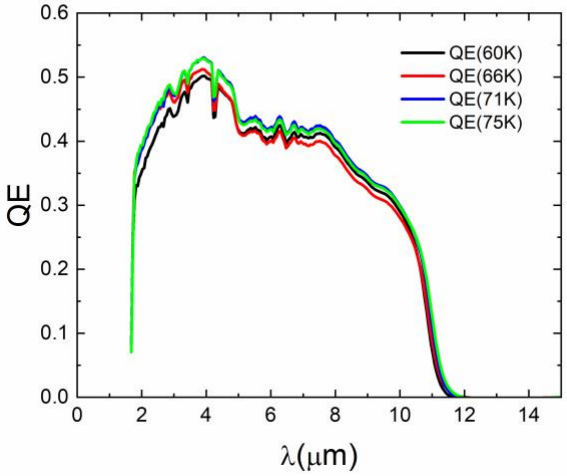

Figure. 8. Backside illuminated spectral QE (no A/R coated) of the HyTI LWIR detector measured at temperatures ranging from 60K to 75K.

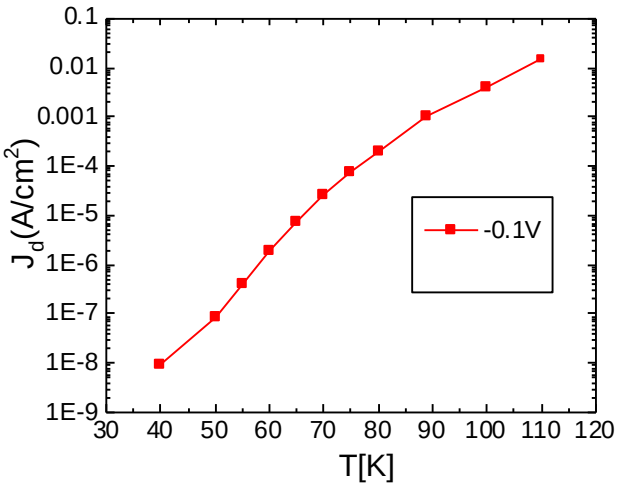

Figure. 9. Dark current density as a function of detector operating temperature at the operating bias of V=-100mV.

Figure 9 shows the measured dark current density as a function of detector operating temperature ranging from 30K to 120K at the operating bias voltage of -100mV. The -50mV dark current density at 70K is 4x10^{-5}A/cm^2. The detector material will be used to fabricate 24μm pitch, 640x512 format arrays and hybridized to the SBF-193 readout integrated circuit (ROIC).

The QE and the noise equivalent temperature difference (NEΔT) provides the thermal sensitivity of an infrared imaging system and it is a very useful diagnostic tool to evaluate the full operational performance available. NEΔT is defined as the minimum temperature difference required at the target to produce unity signal-to-noise-ratio. Sequence of consecutive frames is collected for equivalent noise determination as well as other optical properties of FPA. The photo response matrices of FPA is derived at the low and high blackbody temperatures (i.e., 295 K and 305 K), and temporal noise matrix of FPA is estimated at the mid-point temperature by taking 64 frames of data. The temporal NEΔT of pixels are numerically evaluated from the relations, $NE\Delta T = \sigma_{Temporal}\Delta T/[Mean(T_H) - Mean(T_L)]$. The mean signal $Mean(T_L)$ and $Mean(T_H)$ are evaluated at blackbody temperatures of T_L = 295 K and T_H = 305 K. The temporal noise is measured at 300K using 64 frames, and ΔT ~10 K.

The experimentally measured NEΔT histogram distribution of a 640x512 pixels LWIR trial FPA at 60K operating temperature with blackbody temperature of 300 K and f/4 cold stop is shown in the Figure 10. The experimentally measured NEΔT of 21mK is in fair agreement with the estimated NEΔT value based on the results of a single element test detector data.

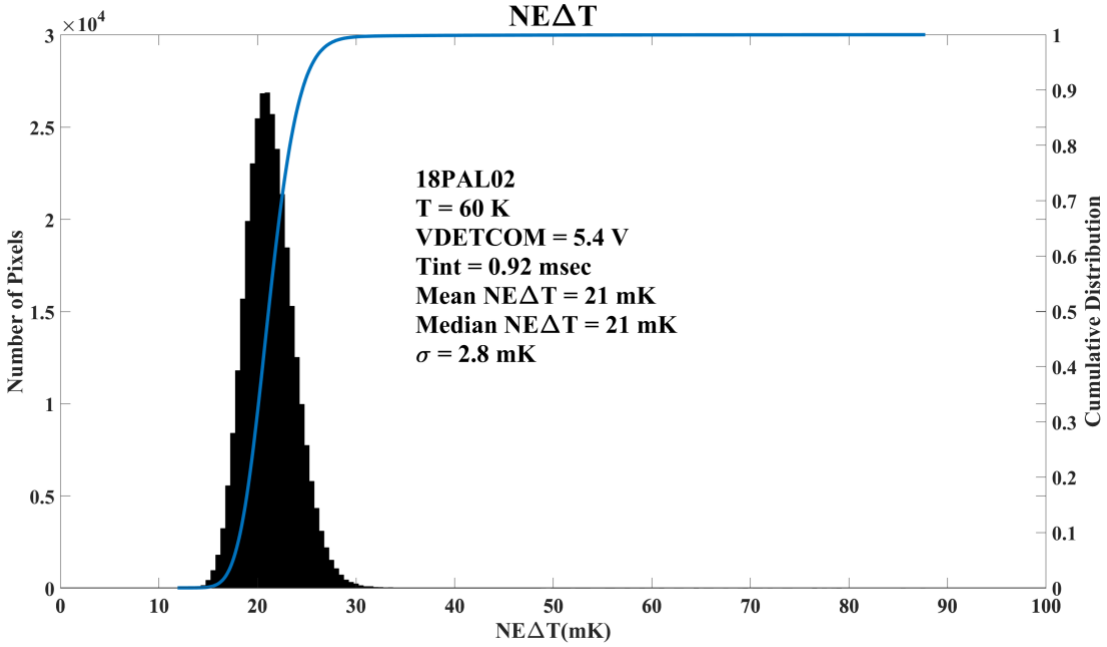

Figure 10. Noise equivalent temperature difference (NEΔT) of a trial 11μm cutoff BIRD FPA at 60K.

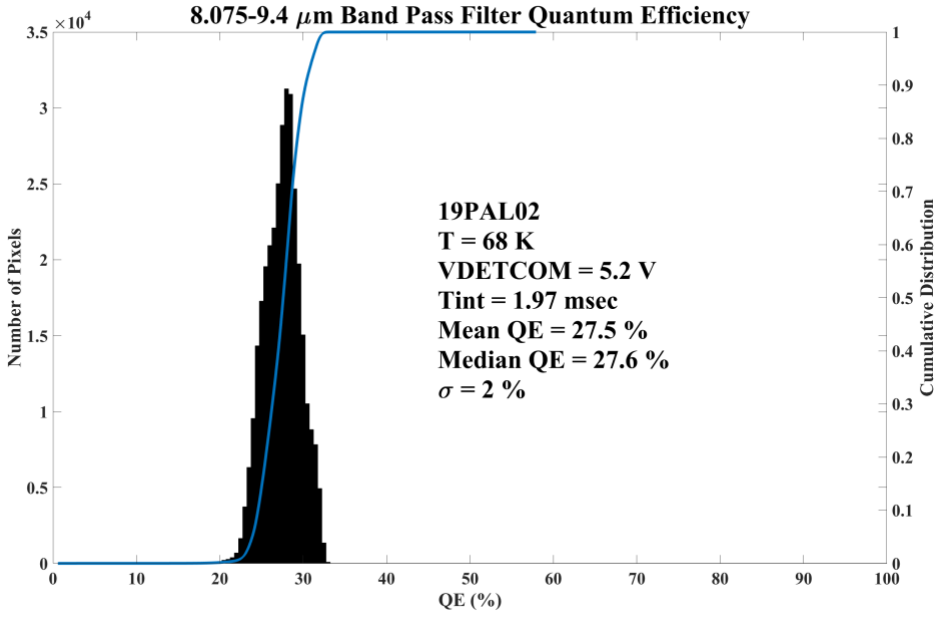

Figure 11. 8-9.4μm broad-bandpass filter QE of a trail LWIR BIRD FPA at 68K.

Wafers	λ_c (μm) at 70K	QE (%) at 9.5μm (No A/R)	QE (%) at 10.5μm (No A/R)	J_d (A/cm^2)
Set 1	11.5	40	37	2E-4
Set 2	10.6	32	21	4E-5
Set 3	11.5	40	35	2E-4

Table 2: Single pixel data of HyTI LWIR BIRD wafers taken with process evaluation chips.

The experimentally measured QE histogram distribution of a 640x512 pixels LWIR trial FPA at 68K operating temperature with blackbody temperature of 300 K and f/4 cold stop is shown in the Figure 11. The experimentally measured FPA QE of 27% is in fair agreement with the estimated QE value based on the results of a single element test detector data. Furthermore, we have grown three more sets of LWIR wafers with the same device architecture. Single element test detectors are already fabricated and characterized and their results are shown in Table 2. These LWIR wafers will be used to fabricate the final LWIR FPA for the HyTI mission.

5. SUMMARY

Ga-free T2SLS MWIR and LWIR BIRD FPAs could easily operate at higher operating temperature (i.e. compared to InSb and QWIP and FPAs) due to the strong suppression of G-R dark current due to SRH processes as explained earlier. We have successfully fabricated MWIR HOT-BIRD FPA and integrated with a dewar cooler assembly for CIRAS 6U CubeSat. We have also successfully fabricated LWIR BIRD FPA for HyTI 6U Cubesat and it will be integrated with a dewar cooler assembly as well. These antimonides based T2SLS BIRDs outperform existing thermal infrared detectors such as Quantum Well Infrared Photodetectors (QWIPs) and InSb. Another 20-30K higher operating temperature advantage can be achieved when we further improve the performance by hybridizing the T2SLS LWIR BIRD detector array to the high-dynamic range in-pixel digital ROICs. Based on III-V compound semiconductors, the T2SL BIRDs offer a breakthrough solution for the realization of low cost (high yield), highperformance FPAs with excellent uniformity and pixel-to-pixel operability. Therefore, T2SLS MWIR and LWIR BIRD FPA technology is very attractive to Earth and planetary remote sensing instruments.

ACKNOWLEDGEMENT

The authors thank the NASA Earth Science Technology Office and Jason Hyon, Eastwood Im, Nikzad, Toomarian, and Harish Manohara of the Jet Propulsion Laboratory for encouragement and support. The research was carried out at the Jet Propulsion Laboratory, California Institute of Technology, under a contract with the National Aeronautics and Space Administration (80NM0018D004).

REFERENCES

1. Sarath Gunapala, David Ting, Cory Hill, and Sumith Bandara, “nBn and pBp infrared detectors with graded barrier layer, graded absorption layer, or chirpped strained layer superlattice absorption layer”, US Patent No. US 7,737,411 B2, June 15, 2010.
2. David Z. Ting, Arezou Khoshakhlagh, Alexander Soibel, Cory J. Hill, and Sarath D. Gunapala, “Barrier infrared detector”, US Patent No. US 8,217,480 B2, July 10, 2012.
3. D. Z. Ting, A. Soibel, A. Khoshakhlagh, S. B. Rafol, S. A. Keo, L. Höglund, A. M. Fisher, E. M. Luong, and S. D. Gunapala, “Mid-wavelength high operating temperature barrier infrared detector and focal plane array”, Appl. Phys. Lett. 113, 021101 (2018). doi: 10.1063/1.5033338
4. Thomas S. Pagano, Carlo Abesamis, Andres Andrade, Hartmut H. Aumann, Sarath D. Gunapala, Cate Heneghan, Robert F. Jarnot, Dean L. Johnson, Andrew Lamborn, Yuki Maruyama, Sir B. Rafol, Nasrat A. Raouf, David M. Rider, David Z. Ting, Daniel W. Wilson, Karl Y. Yee, Jerold Cole, William S. Good, Thomas U. Kampe, Juancarlos Soto, Arnold L. Adams, Matt Buckley, Richard Graham, Fred Nicol, Antonios G. Vengel, John Moore, Thomas Coleman, Steve Schneider, Chris Esser, Scott Inlow, Devon Sanders, Karl Hansen, Matt Zeigler, Charles Dumont, Rebecca Walter, Joe Piacentine, “Technology development in support of hyperspectral infrared atmospheric sounding in a CubeSat”, Proc. SPIE 10769, 1076906 (2018) https://doi.org/10.1117/12.2320911
5. Robert Wright, Miguel Nunes, Paul Lucey, Luke Flynn, Sarath Gunapala, David Ting, Sir Rafol, Alexander Soibel, Chiara Ferrari-Wong, Andrea Gabrieli, Prasad Thenabail, "HYTI: thermal hyperspectral imaging from a CubeSat platform," Proc. SPIE 11131, CubeSats and SmallSats for Remote Sensing III, 111310G (30 August 2019); doi: 10.1117/12.2530821.
6. Sarath Gunapala, Sir Rafol, David Ting, Alexander Soibel, Arezou Khoshakhlagh, Sam Keo, Brian Pepper, Anita Fisher, Cory Hill, Kwong-Kit Choi, Arvind D'Souza, Christopher Masterjohn, Sachidananda Babu, Parminder Ghuman, "T2SL meta-surfaced digital focal plane arrays for Earth remote sensing applications," Proc. SPIE 11129, Infrared Sensors, Devices, and Applications IX, 111290C (9 September 2019); doi: 10.1117/12.2533477.